

Original Article

Endobronchial ultrasound-guided transbronchial needle aspiration of hilar and mediastinal lymph nodes detected on ¹⁸F-fluorodeoxyglucose positron emission tomography/computed tomography

Daisuke Minami^{1,*}, Nagio Takigawa², Naohiro Oda¹, Takashi Ninomiya¹, Toshio Kubo¹, Kadoaki Ohashi¹, Akiko Sato¹, Katsuyuki Hotta¹, Masahiro Tabata¹, Mitsumasa Kaji³, Mitsune Tanimoto¹, and Katsuyuki Kiura¹

¹Department of Respiratory Medicine, Okayama University Hospital, Okayama, ²Department of General Internal Medicine 4, Kawasaki Medical School, Okayama, and ³Okayama Diagnostic Imaging Center, Okayama, Japan

*For reprints and all correspondence: Department of Hematology, Oncology, and Respiratory Medicine, Okayama University Hospital, Okayama 700-8558, Japan. E-mail: d-minami@bj8.so-net.ne.jp

Received 18 September 2015; Accepted 9 February 2016

Abstract

Objective: Endobronchial ultrasound-guided transbronchial needle aspiration is of diagnostic value in hilar/mediastinal (N1/N2) lymph node staging. We assessed the utility of endobronchial ultrasound-guided transbronchial needle aspiration in lung cancer patients with N1/N2 lymph nodes detected on ¹⁸F-fluorodeoxyglucose positron emission tomography/computed tomography.

Methods: Fifty lung cancer patients with N1/N2 disease on ¹⁸F-fluorodeoxyglucose positron emission tomography/computed tomography underwent endobronchial ultrasound-guided transbronchial needle aspiration for pathological lymph nodes between November 2012 and April 2015. The diagnostic performance of endobronchial ultrasound-guided transbronchial needle aspiration, lymph node site and size, number of needle passes and complications were evaluated retrospectively from patients' medical records. Malignancy was defined as a maximum standardized uptake value (SUV_{max}) >2.5.

Results: The median longest diameter of the 61 lymph nodes (29 subcarinal, 21 right lower paratracheal, 6 left lower paratracheal, 4 right hilar and 1 upper paratracheal) was 23.4 mm (range: 10.4–45.7); the median number of needle passes was 2 (range: 1–5). There were no severe complications. A definitive diagnosis was made by endobronchial ultrasound-guided transbronchial needle aspiration in 39 patients (31 adenocarcinomas, 3 small-cell carcinomas, 2 squamous-cell carcinomas, 3 large-cell neuroendocrine carcinomas). In the remaining 11 patients, the diagnosis was indefinite: insufficient endobronchial ultrasound-guided transbronchial needle aspiration material was collected in two patients and non-specific lymphadenopathy was confirmed by endobronchial ultrasound-guided transbronchial needle aspiration or thoracotomy in the other nine patients. The mean lymph node SUV_{max} was 7.09 (range: 2.90–26.9) and was significantly higher in true-positive than in false-positive nodes ($P < 0.05$, t -test). Non-specific lymphadenopathy was diagnosed by expert visual interpretation of ¹⁸F-fluorodeoxyglucose positron emission tomography/computed tomography images in five of the nine patients.

Conclusion: Endobronchial ultrasound-guided transbronchial needle aspiration accurately diagnoses N1/N2 disease detected on ^{18}F -fluorodeoxyglucose positron emission tomography/computed tomography.

Key words: endoscopy-respiratory tract, radiology-PET, lung-RadOncol, endobronchial ultrasound-guided transbronchial biopsy, lung cancer, ^{18}F -fluorodeoxyglucose positron emission tomography/computed tomography

Introduction

^{18}F -fluorodeoxyglucose positron emission tomography/computed tomography (FDG-PET/CT) has been used in the diagnosis of lung cancer and plays a crucial role in distinguishing benign from malignant pulmonary and lymph node lesions. However, its high false-positive rates remain problematic (1). Non-neoplastic lesions with excessive ^{18}F -FDG uptake are typically those with a large number of macrophages and lymphocytes, such as tuberculosis and other granulomas (2). Thus, tissue confirmation is recommended even when the FDG-PET/CT findings in regional lymph nodes are positive (3).

Endobronchial ultrasound-guided transbronchial needle aspiration (EBUS-TBNA) is a minimally invasive procedure with a high diagnostic yield for mediastinal lymph node staging, not only in patients with lung cancer but also in those with other pulmonary and mediastinal diseases (4,5). The American College of Chest Physicians recommends a needle technique [EBUS-needle aspiration, esophageal endoscopic ultrasound-needle aspiration (EUS-NA) or combined EBUS/EUS-NA] over surgical staging as a best first examination in patients in whom N2 and N3 involvement is suspect, based on either discrete mediastinal lymph node enlargement or FDG uptake (6). However, the superiority of EBUS-TBNA over FDG-PET/CT for pre-operative N1/N2 staging has yet to be convincingly documented. Here, we describe our experience using EBUS-TBNA in lung cancer patients with N1/N2 disease detected on FDG-PET/CT.

Patients and methods

Patients

The medical records of 50 consecutive lung cancer patients with N1/N2 disease on FDG-PET/CT were retrospectively evaluated. Between November 2012 and April 2015, all patients with positive lymph nodes on FDG-PET/CT underwent EBUS-TBNA for further diagnosis of pathological lymph nodes. EBUS-TBNA and FDG-PET/CT were performed at Okayama University Hospital and Okayama Diagnostic Imaging Center, respectively. A maximum standardized uptake value (SUV_{max}) >2.5 was defined as a positive result signifying malignancy. The study was approved by the Institutional Ethics Committee of Okayama University Hospital (no. 1508-019).

^{18}F -fluorodeoxyglucose positron emission tomography

Blood glucose was measured in fasted (≥ 5 h) patients to ensure a level of <140 mg/dl. Patients were then administered an intravenous injection of 3.7 MBq FDG/kg (1.0×10^{-4} Ci/kg) body weight and asked to rest in a reclining chair until the scan, to minimize muscle consumption of FDG. PET image acquisition using an integrated PET/CT scanner (Biograph LS/Sensation16, Siemens, Munchen, Germany) began 90 min after the injection of FDG. Scanning was performed with the patient in a relaxed supine position. First, a total-body low-dose CT scan was acquired to calculate the attenuation correction. The standardized protocol was as follows: 140 kV, 12–14 mAs, a tube-rotation

time of 0.5 s per rotation, a pitch of 0.8, a section thickness of 3 mm and a scan field ranging from the head to the mid-thigh level (7–8 bed positions, 2.4 min per table position). The PET images were reconstructed with an ordered-subset expectation maximization iterative reconstruction algorithm. Integrated, coregistered PET/CT images were obtained using a workstation (PET Viewer, AZE, Tokyo, Japan), which enabled image fusion and analysis. Expert visual interpretation of the images by radiologists specialized in PET/CT was obtained before bronchoscopic examination of the patients. In expert visual interpretation by radiologists, the clinical applicability of lymph node enlargement in CT is >10 mm short axis diameter. Additionally, the shape, grouping, necrosis and extranodal tumor spread were considered. High SUV_{max} in PET was easily defined as a positive result signifying malignancy. Moreover, clinical data were considered (7). Receiver operating characteristic (ROC) curves analysis was used by STATA/SEversion 11.0 software (College Station, TX, USA).

Procedure

All bronchoscopic procedures were performed on an in-patient basis. Conventional flexible bronchoscopy (BF-260 Bronchovideoscope, Olympus; Tokyo, Japan) was performed for observational purposes, using a siliconized, uncuffed tracheal tube with an inner diameter of 7.5 mm (Portex; Smiths Medical, St. Paul, MN, USA). EBUS-TBNA was then performed using a convex-probe EBUS bronchoscope (BF-UC260F-OL8, Olympus; Tokyo, Japan). Prior to the latter procedure, the patients were administered 25 mg of hydroxyzine pamoate by intramuscular injection. Of note, 5 ml of 2% lidocaine was first sprayed into the pharynx and then administered again through the working channel during the examination. The bronchoscope was inserted orally in patients under conscious sedation induced by midazolam or a combination of midazolam and fentanyl. Patients were monitored by electrocardiogram, pulse oximetry and blood pressure without the presence of an anesthesiologist. Mediastinal lymph nodes accessible by EBUS (stations 2, 4 and 7) and hilar lymph nodes (stations 10 and 11) were examined to identify those with a $\text{SUV}_{\text{max}} >2.5$.

Specimen handling

The aspirated material was pushed out of the puncture needle, smeared on a watch glass and then evaluated immediately by an on-site cytopathologist using Bioevaluator[®] (Murazumi Industrial Co. Ltd, Osaka, Japan) (8). More than half of the smears were stained using Hemacolor[®] rapid staining (Promiclos; Tokyo, Japan). The remaining samples were fixed in 10% formalin, paraffin-embedded, stained with Papanicolaou stain and evaluated histologically.

Statistical analysis

Statistical analysis was performed using Microsoft Office Excel 2007 (Microsoft Japan Corporation, Tokyo, Japan). Comparisons between the two groups were made using unpaired Student's *t*-test. A *P* value <0.05 was considered to indicate statistical significance.

Results

The patients' characteristics are listed in Table 1. The median age of the 34 males and 16 females was 61 (range, 34–84) years. Peripheral lung nodules were evaluated by bronchoscopy or CT-guided biopsy. The pathological diagnoses were as follows: 36 adenocarcinomas, 8 squamous-cell carcinomas, 3 small-cell carcinomas and 3 large-cell neuroendocrine carcinomas. The lymph nodes ($n = 61$) were subsequently aspirated with a median of 2 (range, 1–5) attempts per node and consisted of 29 subcarinal, 21 right lower paratracheal, 6 left lower paratracheal, 4 right hilar nodes and 1 upper paratracheal node (Table 2). The mean size of the enlarged lymph nodes, measured over the long axis using CT imaging, was 23.4 (range, 10.4–45.7) mm. During EBUS-TBNA, 4 patients experienced fever, which was easily managed. Necrotic or cystic areas in 10 of 61 lymph nodes were punctured, and the patients did not experience fever or severe complications. Device breakage was not observed during this study. The use of EBUS-TBNA allowed for definitive diagnoses in 39 patients (31 adenocarcinomas, 2 squamous-cell carcinomas, 3 small-cell carcinomas and 3 large-cell neuroendocrine carcinomas). Pathological diagnoses could not be made in 11 patients. The EBUS-TBNA samples in 9 of these patients contained abundant lymphocytes, and all 9 underwent a thoracotomy. The resected lymph nodes had normal lymphocytes without malignant cells. Expert visual interpretation of the PET/CT images obtained from these patients was non-specific lymphadenopathy in five cases. The EBUS-TBNA samples in the remaining 2 of

the 11 patients were insufficient for evaluation. In both cases, cancer metastasis was finally diagnosed, because the lymph nodes responded to chemoradiotherapy with a reduction in size. Thus, EBUS-TBNA samples from 48 of the 50 patients were diagnostically sufficient (Supplementary data, Table S1).

The mean SUV_{max} of the lymph nodes from the 50 patients was 7.09 (range, 2.90–26.9). The mean SUV_{max} of the negative lymph nodes diagnosed by EBUS-TBNA or thoracotomy [4.75 (range, 3.11–7.14; $n = 12$)] was significantly lower than that of the positive lymph nodes diagnosed by EBUS-TBNA alone [11.35 (range, 2.90–26.9; $n = 47$)] ($P < 0.05$). The SUV_{max} of the lymph nodes from the two patients with insufficient material was 2.99 and 8.79. We showed sensitivity, specificity, positive predict value, negative predict value and accuracy by EBUS-TBNA and PET-CT were shown in Supplementary data, Table S2. Although $SUV_{max} > 2.5$ was selected for cut-off point in this study, ROC curve of PET/CT according to variable SUV_{max} was described in Supplementary data, Figure S1. In order to predict a more favorable cut-off point of SUV_{max} than 2.5, we calculated the diagnostic accuracy (Supplementary data, Table S3). When the cut-off point was set to 4.31, the diagnostic accuracy was 83.61% with sensitivity of 89.80% and specificity of 58.33%. The prediction cut-off point of SUV_{max} may depend on the histological type. Since most predominant histology was adenocarcinoma, we performed ROC curve analysis (Supplementary data, Figure S2) and calculated diagnostic accuracy, sensitivity, and specificity (Supplementary data, Table S4) in adenocarcinoma histology. The most favorable cut-off point was 4.31 with diagnostic accuracy of 80.00%, sensitivity of 86.84% and specificity of 58.33%.

A representative case is shown in Fig. 1. A 58-year-old male with lung cancer in the right middle lobe had mediastinal lymph node enlargement with FDG uptake. The SUV_{max} was 3.72. Expert visual interpretation resulted in a diagnosis of metastasis; however, the EBUS-TBNA samples contained abundant lymphocytes without malignant cells. Evaluation of the surgically resected lymph node revealed non-specific lymphadenopathy.

Discussion

Although this was a small and retrospective study, our experience has shown that EBUS-TBNA is useful for diagnosing N1/N2 disease detected on FDG-PET/CT. The superiority of EBUS-TBNA over FDG-PET/CT for preoperative N1/N2 staging was previously suggested (9,10), although it could not be definitively documented. FDG-PET/CT plays a crucial role in detecting mediastinal lymph node involvement in patients with potentially resectable lung cancer. However, its sensitivity and specificity are too low for mediastinal staging (0.77–0.81 and 0.79–0.90, respectively) (11). Our results, reported in Table 2, are in agreement with this conclusion, as only 78% (39/50) of the study patients with N1/N2 disease detected on FDG-PET/CT ($SUV_{max} > 2.5$) were similarly diagnosed by EBUS-TBNA, whereas the 9 patients with N2 disease on FDG-PET/CT underwent surgical treatment based on the number of normal lymphocytes in their EBUS-TBNA samples, which indicated benign lymphadenopathy.

The utility of EBUS-TBNA for preoperative lymph node staging in patients with lung cancer is widely accepted, and the procedure is at least as effective as mediastinoscopy for the mediastinal staging of non-small-cell lung cancer, given its high sensitivity (~90%) and specificity (~100%) (12–14). In this study, EBUS-TBNA samples of 96% (48/50) of the patients contained a sufficient number of lymphocytes to allow a diagnosis. Based on expert visual interpretation of the FDG-PET/CT images, non-specific lymphadenopathy was diagnosed

Table 1. Patient characteristics

Characteristic	Value (range)
Number of patients	50
Male/female, n	34/16
Median age (range), years	61 (34–84)
Pathological diagnosis, n	
Adenocarcinoma	36
Squamous-cell carcinoma	8
Small-cell carcinoma	3
Large-cell neuroendocrine carcinoma	3

Table 2. Characteristics of the punctured lymph nodes

Characteristic	Value (range)
Number	61
Enlarged lymph node stations ^a (4R/4L/7/11/2R), n	21/6/29/4/1
Longest diameter (range), mm	23.4 (10–45)
Diagnosis by EBUS-TBNA, n	
Adenocarcinoma	31
Squamous-cell carcinoma	2
Small-cell carcinoma	3
Large-cell neuroendocrine carcinoma	3
Indefinite	11
Mean SUV_{max} (range)	7.09 (2.90–26.9)
Positive nodes by EBUS-TBNA ($n = 47$)	11.35 (2.90–26.9)
Negative nodes by EBUS-TBNA or thoracotomy ($n = 12$)	4.75 (3.11–7.14)
Uncertain nodes by EBUS-TBNA ($n = 2$)	5.79 (2.99–8.79)

EBUS-TBNA, endobronchial ultrasound-guided transbronchial needle aspiration; SUV, standardized uptake value.

^aLymph node stations were defined as follows: 4L, left lower paratracheal node; 4R, right lower paratracheal node; 7, subcarinal nodes; 11, N1 nodes; 2R, upper paratracheal node.

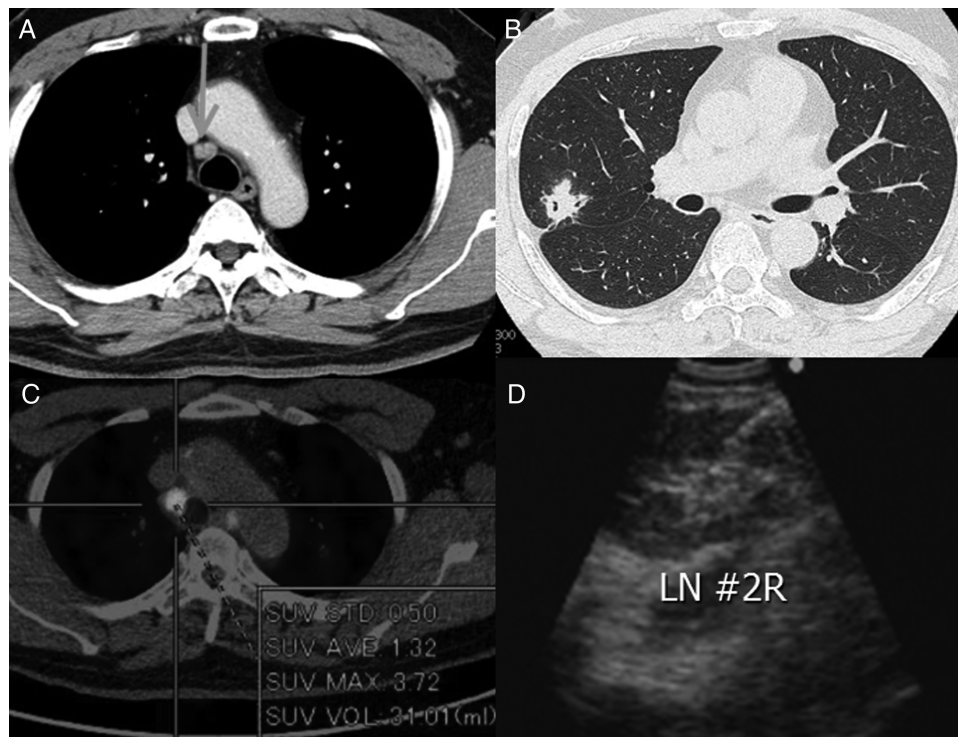


Figure 1. A 58-year-old male patient with lung cancer in the right middle lobe had mediastinal lymph node enlargement on computed tomography (CT) (A and B), positron emission tomography/computed tomography (PET/CT) (C) and endobronchial ultrasound (D) imaging.

in five of the nine patients whose EBUS-TBNA samples showed normal lymphocytes without malignant cells. Thus, EBUS-TBNA can be considered as a diagnostic tool regardless of expert visual interpretation. The first Japanese nationwide survey describing complications associated with the use of EBUS-TBNA revealed severe infections and frequent device breakages (15). Although necrotic or cystic areas in 10 of 61 lymph nodes were punctured, we did not experience fever and severe complications in such cases. Device breakage was not observed during this study. However, we should take care to avoid severe complications and device breakage.

The threshold of SUV_{max} for positive lymph nodes has yet to be definitively defined. In our patients, positive lymph nodes had a significantly higher mean SUV_{max} than negative lymph nodes, as subsequently determined by EBUS-TBNA (Table 2). We have also seen patients with negative mediastinal findings ($SUV_{max} < 2.5$) on FDG-PET/CT whose EBUS-TBNA samples included malignant cells. Thus, studies aimed at determining the threshold SUV_{max} to identify those patients who are candidates for EBUS-TBNA would be highly valuable. Among the many factors that contribute to the SUV are body mass including fat tissue (16), blood glucose level (17), time of the examination in relation to administration of the marker and the size of the lesion (18). Recently, several different objective criteria for FDG-PET/CT scan interpretation were proposed: SUV_{max} lymph node/ SUV_{max} primary lung malignancy (19), SUV_{max} lymph node/ SUV_{max} average liver (20), SUV_{max} lymph node/ SUV_{max} liver (21), and SUV_{max} lymph node/ SUV_{max} blood pool (22). Schmidt-Hansen et al. (11) reported that the sensitivity and specificity of FDG-PET/CT were related not only to the FDG dose but also to other factors. Since most favorable predictive cut-off point of SUV_{max} in not only all histology but also adenocarcinoma alone was 4.31 in this study, we should evaluate the value prospectively. The cut-off point or the other objective criteria for PET/CT scan interpretation (19–22)

might be useful for estimating lymph nodes which are difficult to obtain by EBUS-TBNA. Further prospective studies will aid in determining the objective criteria for FDG-PET/CT scan interpretation and therefore whether N1/N2 staging with EBUS-TBNA is more accurate.

Conclusion

EBUS-TBNA may be useful in classifying benign and malignant N1/N2 disease detected on FDG-PET/CT and should be considered for accurate staging in patients with lung cancer and lymph node involvement.

Supplementary data

Supplementary data are available at <http://www.jjco.oxfordjournals.org>.

Acknowledgements

We thank cytoscreener, Mr Hirofumi Inoue, and Drs Go Makimoto, Hiromi Watanabe, Masamoto Nakanishi, Yusuke Hata, Kiichiro Ninomiya and Hirohisa Kano for performing the bronchoscopies and for the helpful discussions. This study was supported in part by a Grant-in-Aid for Young Scientists (B), Culture, Sport, Science, and Technology, Japan (15K2118507). The English in this document has been checked by at least two professional editors, both native speakers of English. For a certificate, please see: <http://www.textcheck.com/certificate/eyybQJ>.

Funding

Funding to pay the Open Access publication charges for this article was provided by the Ministry of Education, Culture, Sports, Science, and Technology, Japan (15K21185).

Conflict of interest statement

None declared.

References

- Verhagen AF, Bootsma GP, Tjan-Heijnen VC, van der Wilt GJ, Cox AL, Brouwer MH, et al. FDG-PET in staging lung cancer: how does it change the algorithm? *Lung Cancer* 2004;44:175–81.
- Bakheet SM, Saleem M, Powe J, Al-Amro A, Larsson SG, Mahassin Z. F-18 fluorodeoxyglucose chest uptake in lung inflammation and infection. *Clin Nucl Med* 2000;25:273–8.
- Detterbeck FC, Jantz MA, Wallace M, Vansteenkiste J, Silvestri GA. Invasive mediastinal staging of lung cancer: ACCP evidence-based clinical practice guidelines (2nd edition). *Chest* 2007;132:202S–220S.
- Nakajima T, Yasufuku K. How I do it – Optimal methodology for multidirectional analysis of endobronchial ultrasound-guided transbronchial needle aspiration samples. *J Thorac Oncol* 2011;6:203–6.
- Fernández-Bussy S, Labarca G, Canals S, Caviedes I, Folch E, Majid A. Diagnostic yield of endobronchial ultrasound-guided transbronchial needle aspiration for mediastinal staging in lung cancer. *J Bras Pneumol* 2015;41:219–24.
- Silvestri GA, Gonzalez AV, Jantz MA, Margolis ML, Gould MK, Tanoue LT, et al. Methods for staging non-small cell lung cancer: Diagnosis and management of lung cancer, 3rd edn. American College of Chest Physicians evidence-based clinical practice guidelines. *Chest* 2013;143:e211S–50.
- Keidar Z, Haim N, Guralnik L, Wollner M, Bar-Shalom R, Ben-Nun A, et al. PET/CT Using 18F-FDG in suspected lung cancer recurrence: diagnostic value and impact on patient management. *J Nucl Med* 2004;45:1640–6.
- Minami D, Takigawa N, Inoue H, Hotta K, Tanimoto M, Kiura K. Rapid on-site evaluation with BIOEVALUATOR[®] during endobronchial ultrasound-guided transbronchial needle aspiration for diagnosing pulmonary and mediastinal diseases. *Ann Thorac Med* 2014;9:14–7.
- Cornwell LD, Bakaeen FG, Lan CK, Omer S, Preventza O, Pickrell B, et al. Endobronchial ultrasonography-guided transbronchial needle aspiration biopsy for preoperative nodal staging of lung cancer in a veteran population. *JAMA Surg* 2013;148:1024–9.
- Shingyoji M, Nakajima T, Yoshino M, Yoshida Y, Ashinuma H, Itakura M, et al. Endobronchial ultrasonography for positron emission tomography and computed tomography-negative lymph node staging in non-small cell lung cancer. *Ann Thorac Surg* 2014;98:1762–7.
- Schmidt-Hansen M, Baldwin DR, Zamora J. FDG-PET/CT imaging for mediastinal staging in patients with potentially resectable non-small cell lung cancer. *JAMA* 2015;313:1465–6.
- Ernst A, Anantham D, Eberhardt R, Krasnik M, Herth FJ. Diagnosis of mediastinal aspiration versus mediastinoscopy. *J Thorac Oncol* 2008;3:577–82.
- Gu P, Zhao YZ, Jiang LY, Zhang W, Xin Y, Han BH. Endobronchial ultrasound-guided transbronchial needle aspiration for staging of lung cancer: a systematic review and meta-analysis. *Eur J Cancer* 2009;45:1389–96.
- Yasufuku K, Nakajima T, Motoori K, Sekine Y, Shibuya K, Hiroshima K, et al. Comparison of endobronchial ultrasound, positron emission tomography, and CT for lymph node staging of lung cancer. *Chest* 2006;130:710–8.
- Asano F, Aoe M, Ohsaki Y, Okada Y, Sasada S, Sato S, et al. Bronchoscopic practice in Japan: a survey by the Japan Society for Respiratory Endoscopy in 2010. *Respirology* 2013;18:284–90.
- Zasadny K, Wahl R. Standardized uptake values of normal tissues at PET with 2-[fluorine-18]-fluoro-2-deoxy-D-glucose: variations with body weight and a method for correction. *Radiology* 1993;189:847–50.
- Lindholm P, Minn H, Leskinen-Kallio S, Bergman J, Ruotsalainen U, Joensuu H. Influence of the blood glucose concentration on FDG uptake in cancer: a PET study. *J Nucl Med* 1993;34:1–6.
- Hamberg L, Hunter G, Alpert N, Choi N, Babich J, Fischman A. The dose uptake ratio as an index of glucose metabolism: useful parameter or oversimplification? *J Nucl Med* 1994;35:1308–12.
- Zielonka T, Pietrzykowski J, Wardyn K. PET-CT in evaluation of pulmonary nodule—case report. *Pol Merk Lek* 2009;158:119–22.
- Cerfolio RJ, Bryant AS. Ratio of the maximum standardized uptake value on FDG-PET of the mediastinal (N2) lymph nodes to the primary tumor may be a universal predictor of nodal malignancy in patients with non-small-cell lung cancer. *Ann Thorac Surg* 2007;83:1826–9.
- Tournoy KG, Maddens S, Gosselin R, Van Maele G, van Meerbeeck JP, Kelles A. Integrated FDG-PET/CT does not make invasive staging of the intrathoracic lymph nodes in non-small cell lung cancer redundant: a prospective study. *Thorax* 2007;62:696–701.
- Gupta NC, Graeber GM, Bishop HA. Comparative efficacy of positron emission tomography with fluorodeoxyglucose in evaluation of small (<1 cm), intermediate (1 to 3 cm), and large (>3 cm) lymph node lesions. *Chest* 2000;117:773–8.